



Share Your Innovations through JACS Directory

Journal of Nanoscience and Technology

Visit Journal at <http://www.jacsdirectory.com/jnst>

Synthesis and Characterization of Cobalt Oxide Nanoparticles

K. Prema Latha^{1,*}, C. Prema², S. Meenakshi Sundar²¹Research Scholar (Reg. No. 11639), PG and Research Department of Physics, Sri Paramakalyani College, Alwarkurichi, Affiliated to Manonmaniam Sundaranar University, Abishekapatti, Tirunelveli – 627 012, Tamil Nadu, India.²PG and Research Department of Physics, Sri Paramakalyani College, Alwarkurichi, Tirunelveli – 627 412, Tamil Nadu, India.

ARTICLE DETAILS

Article history:

Received 16 July 2018

Accepted 25 July 2018

Available online 20 August 2018

Keywords:

Cobalt Oxide

Supercapacitor

Microwave

Williamson-Hall Plot

ABSTRACT

The present work reports the synthesis and characterization of cobalt oxide nanoparticles. Microwave oven method was used for synthesizing cobalt oxide nanoparticles. The synthesized nanoparticles were characterized by X-ray diffraction (XRD), Fourier transform infrared spectroscopy (FT-IR), UV-Vis spectroscopy, photoluminescence (PL) and scanning electron microscope (SEM). The prepared samples show poor crystalline nature so that the samples were calcined at 300 °C for 1 hr. The calcined samples were characterized for further changes in its morphology. XRD identifies the sample is in Co₃O₄ phase with face-centered cubic structure. Debye-Scherrer formula was used to calculate the average crystallite size of the annealed sample and it was found to be 7 to 28 nm. In addition to crystallite size, specific surface area, dislocation density and microstrain are calculated using XRD. Williamson-Hall plot was used to calculate the size and strain. FT-IR spectrum shows two stretching bands at 660 and 550 cm⁻¹ which confirm the functional group present in the cobalt oxide nanoparticles. In optical absorption studies, a blue shift in the energy band gap reveals the quantum confinement effect. Photoluminescence spectra shows emission peak in the visible region.

1. Introduction

Spinel-type cobalt oxide (Co₃O₄) is a transition metal oxide, it has the most stable phase in the Co-O system. It is a mixed valence compound [Co^{II}Co^{III}₂O₄] with a normal spinel structure in which Co(II) ions occupy the tetrahedral 8a sites and Co(III) ions occupy the octahedral 16d sites [1-4]. Co₃O₄ is technologically important material with wide range of applications in lithium ion batteries, heterogeneous catalysts, gas sensing, ceramic pigments, electrochemical devices and it can also be used as a selective coating material for high-temperature solar collectors as these cobalt oxide coatings are very much superior to the black chrome coatings in solar collectors [5]. In recent days Co₃O₄ has attained great interest for its application in supercapacitors. Due to the ability to deliver higher power density than batteries, supercapacitors receive more attention in recent years. Supercapacitors are used in many applications such as mobile phones, digital cameras and solar cell power storage. Some materials which are used as an electrode material for supercapacitors are metal oxides, metal sulfides etc. Co₃O₄ nanoparticles can also be used as an electrode material for supercapacitors [6].

Co₃O₄ nanoparticles have been synthesized by various methods like sol-gel, surfactant-mediated synthesis, thermal decomposition, polymer-matrix assisted synthesis and spray-pyrolysis [7-9]. For the present study microwave oven method has been used for the synthesis of cobalt oxide nanomaterials since this method has attracted great interest due to its simplicity and it is energy-efficient technique. It has potential advantages including its operational simplicity, synthesizing material in a short period of time, high yield, high purity of the synthesized material, low energy consumption.

2. Experimental Methods

2.1 Materials

All chemicals used in the experiment are analytic reagent grade. Cobalt (II) acetate (tetrahydrated), urea, ethylene glycol and acetone were

purchased from HPLC, India. Deionized water was used throughout the experiment.

2.2 Synthesis

Analar grade cobalt (II) acetate (tetrahydrated), urea, along with ethylene glycol was used for the preparation of cobalt oxide nanocrystals. Cobalt oxide nano particles were synthesised in the following method.

Cobalt (II) acetate and urea were taken in 1:3 molecular ratios, mixed and dissolved in 50 mL of ethylene glycol solvent, using a magnetic stirrer for 1 hr at room temperature. After stirring, a clear transparent solution was obtained. The clear solution was transferred to a ceramic bowl and placed in a domestic microwave oven and special care was taken in the synthesis of the material by maintaining ON time and OFF time of the microwave oven for 30 seconds each throughout the synthesis of the material. Due to microwave heating, solvents were evaporated and a precipitate was formed. The precipitates were carefully collected and washed with deionized water for several times, to remove the ions possibly remaining in the final products, and then, washed with acetone for several times to remove the unwanted organic compounds, if any, present in the synthesized sample and then dried. Since the dried samples show poor crystalline nature, the samples were calcined at 300 °C for 1 hr.

2.3 Spectral Characterization

The crystal structures of the annealed samples were characterized by X-ray Diffraction (XRD) analysis. Morphology and structures were observed by scanning electron microscopy (SEM). The functional groups present in the samples were identified by Fourier transform infrared spectroscopy (FTIR). The optical studies were carried out using UV-Vis and photoluminescence studies.

3. Results and Discussion

3.1 XRD

XRD patterns of the prepared Co₃O₄ nanoparticles show amorphous. The samples were calcined at 300 °C for 1 hr. The XRD of the calcined Co₃O₄ nanoparticles is shown in Fig. 1. XRD pattern shows the cobalt oxide has cubic phase structure. The peak positions (2θ = 31.28°, 36.88°, 59.40° and 65.38° related to the plane of (2, 2, 0), (3, 1, 1), (5, 1, 1) and (4, 4, 0)

*Corresponding Author:premalathapremi@gmail.com(K. Prema Latha)

respectively and relative intensities obtained for the Co_3O_4 nanomaterial match well with the JCPDS card No: 431003, identifying the sample as Co_3O_4 with a face-centered cubic structure with Fd-3m (227) space group. Reported value of lattice constant $a = 8.084 \text{ \AA}$ [10].

The lattice parameter 'a' of Co_3O_4 nanoparticles was found using the following relation [11].

$$a = d_{hkl} (h_2 + k_2 + l_2)^{1/2} \quad (1)$$

The value of 'a' calculated from the XRD pattern is 8.0816 \AA for (311) plane and volume of the unit cell as 527.83 \AA^3 .

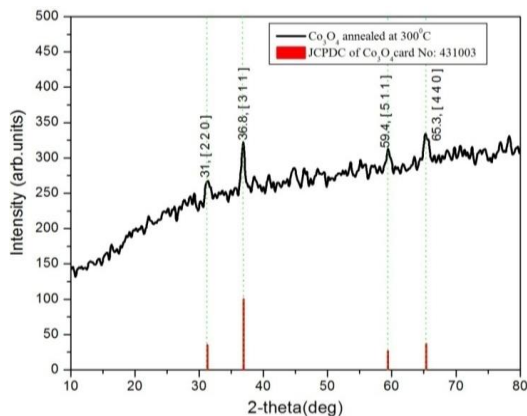


Fig. 1 XRD of Co_3O_4 nanoparticles prepared at $300 \text{ }^\circ\text{C}$

The average crystallite size of Co_3O_4 is determined using Debye-Scherrer relation [12], $D = K\lambda/\beta\cos\theta$, where, β is the full width half maximum in radian, θ is the scattering angle, λ is the X-ray wavelength of radiation with 1.54 \AA , K is the correction factor and D is the crystallite size of material in nm. Then substituting the values in Debye-Scherrer equation, the crystallite size of Co_3O_4 are found to be around 28.37 nm for (311) plane.

The strongest peak (311) was used to estimate the lattice expansion of the nanocrystals. A small lattice contraction along the (220) and (511) was observed in the Co_3O_4 this lattice contraction is due to the lattice strain induced due to large surface/volume ratio. Jiang et al. discussed that decrease in size is responsible for the lattice contraction [13, 14]. The percentage of contraction for each plane is given in Table 1.

Table 1 Lattice contraction for different planes

2 θ (deg)	hkl	d_{XRD} (\AA)	d_{JCPDS} (\AA)	% of contraction in d	FWHM (deg)	Lattice parameter 'a' (nm)	D (nm)
31.2873	220	2.8589	2.8580	-0.0315	0.5904	8.0864	13.97
36.8888	311	2.4367	2.4374	0.0287	0.2952	8.0816	28.37
59.4094	511	1.5557	1.5558	0.0064	1.1808	8.0841	7.75
65.3862	440	1.4272	1.4291	0.1329	0.5904	8.0739	15.99

X-ray density for a cubical system can be calculated from Eq.(2)[14],

$$D_x = 8M/Na^3 \quad (2)$$

where M is the molecular weight, N is Avogadro's constant and 'a' the lattice constant. The calculated value of X-ray density, D_x is 6.05988 g/cm^3 . The specific surface area of the Co_3O_4 nanocrystals along the strongest peak (311) can be calculated using the X-ray density and the particle size by using the formula:

$$Sa = 6/DD_x \quad (3)$$

where, D and D_x are the particle size and X-ray density of the Co_3O_4 nanocrystals respectively. The calculated value of specific surface area is $35.36 \times 10^4 \text{ cm}^2/\text{g}$.

Microstrains are very common in nanocrystalline materials, the peak broadening due to microstrain [12] will vary as:

$$\beta(2\theta) = 4\epsilon \tan(\theta) \quad (4)$$

where, β is the full width half maximum in radian; θ is the scattering angle; ϵ is the micro strain.

The dislocation density (δ), which represents the amount of defects in the sample is defined as the length of dislocation lines per unit volume of the crystal and is calculated using Williamson and Smallman relation [15],

$$\delta = 1/D^2 \quad (5)$$

where, D is the crystallite size. Crystallite size, specific surface area, dislocation density and micro strain are calculated for different planes and it is given in Table 2.

Table 2 Structural parameters of Co_3O_4 nanoparticles

2 θ (deg)	FWHM	h, k, l	Lattice parameter 'a' (nm)	D (nm)	D_x (g/cm^3)	Sa 10^4 (cm^2/g)	Dislocation density ($10^{-4} \text{ (nm)}^{-2}$)	Strain (ϵ)
31.28	0.5904	2, 2, 0	8.0864	13.97	6.0486	71.01	51.23	0.5270
36.88	0.2952	3, 1, 1	8.0816	28.37	6.0598	35.36	12.42	0.2212
59.41	1.1808	5, 1, 1	8.0841	7.75	6.0540	127.88	166.4	0.5174
65.38	0.5904	4, 4, 0	8.0739	15.99	6.0767	61.75	39.11	0.2299

3.2 Williamson-Hall Technique

Williamson and Hall plot is a classical method to obtain qualitative information of anisotropy in broadening. Williamson and Hall [16] assumed that both size and strain broadened profiles are Lorentzian. Based on this assumption, a mathematical relation was established between the integral breadth (β), volume weighted average domain size (D) and the microstrain (ϵ) as follows.

$$\frac{\beta \cos \theta}{\lambda} = \frac{1}{D} + 2\epsilon \left(\frac{2 \sin \theta}{\lambda} \right) \quad (6)$$

The plot shown in Fig. 2 of $\frac{\beta \cos \theta}{\lambda}$ versus $\left(\frac{4 \sin \theta}{\lambda} \right)$ gives the value of the microstrain from the slope and crystallite size from the ordinate intercept. The points in the Williamson-Hall plot are scattered, i.e., $\frac{\beta \cos \theta}{\lambda}$ is not a monotonous function of $\left(\frac{4 \sin \theta}{\lambda} \right)$, the broadening is termed as anisotropic.

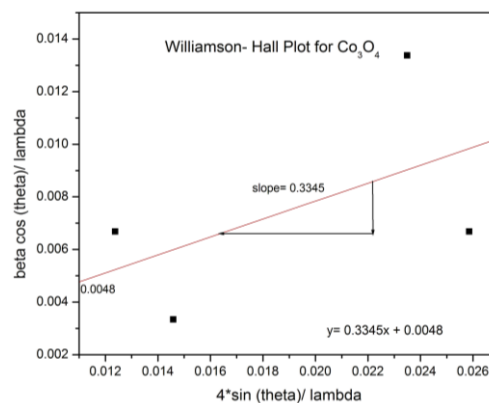


Fig. 2 Williamson-Hall plot for Co_3O_4

Bragg peak position and the full width-half maximum, and the wavelength of incident X-ray were used to evaluate lattice micro strain with the Williamson-Hall method [16]. In this study, four peaks; (2, 2, 0), (3, 1, 1), (5, 1, 1) and (4, 4, 0) were used. The crystallite size calculated from Williamson-Hall plot was 20.88 nm and strain is 0.3345 .

3.3 FT-IR Studies

FT-IR spectrum of Co_3O_4 nanoparticles (Fig. 3) showed significant absorption peaks at 660 and 550 cm^{-1} .

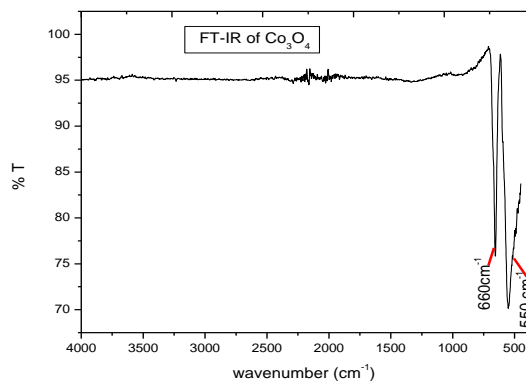


Fig. 3 FT-IR spectrum of Co_3O_4 annealed at $300 \text{ }^\circ\text{C}$

The absorption band at 550 cm^{-1} was assigned to Co-O stretching vibration mode and 660 cm^{-1} was assigned to the bridging vibration of O-

Co-O bond [17]. The 660 cm^{-1} band is characteristic of Co^{2+} -O vibration in a tetrahedral site, and the band 550 cm^{-1} is attributable to the Co^{3+} -O vibration in an octahedral site of the Co_3O_4 lattice [18].

3.4 Optical Studies - UV- Vis and PL Studies

The UV-Vis spectroscopy studies show absorption peaks at 206.4 nm and 210.4 nm. These absorption peaks are blue shifted when compared with the bulk material. The optical band gap becomes larger as the particle size decreases as observed by other investigators [19, 20]. However, nanosized semiconductors display a blue shift in their spectra, due to the quantum confinement effects and/or lattice contraction [20, 21]. The UV-vis spectrum shows the exciton energy at 6.01 eV and 5.89 eV.

Photoluminescence shows peaks at 459 and 484 nm shown in Fig. 4. The emission in the UV region is due to the free excitons and the emission is in the visible region. This is due to the impurities and structural defects in the nanocrystal [6, 22].

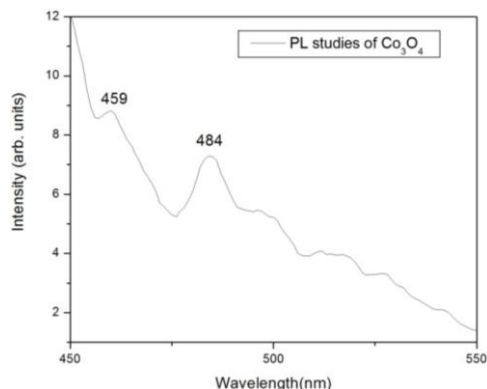


Fig. 4 PL spectrum of Co_3O_4

3.5 SEM

SEM micrograph of the Co_3O_4 calcinated at 300 °C is shown in Fig. 5. It can be seen that the particles are spherical in morphology and are evenly sized. The particles are agglomerated at the surface. The agglomerates were purely due to the magnetic induction between the particles [7, 23].

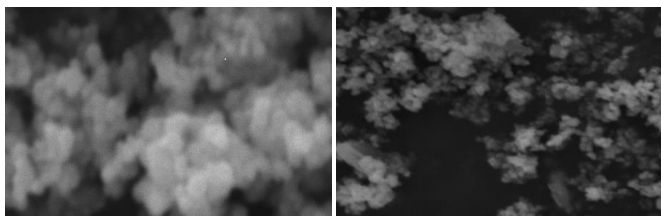


Fig. 5 SEM morphological images of Co_3O_4

4. Conclusion

Microwave irradiation has yielded nanosized Co_3O_4 with fcc spinel structure. The average particle size of Co_3O_4 was 7–28 nm was calculated from Debye-Scherrer formula. The size and strain from the Williamson-Hall plot was 20.88 nm and 0.3345 respectively. FT-IR analysis confirms the presence of Co-O bond [$[\text{Co}^{\text{II}}\text{Co}^{\text{III}}_2\text{O}_4]$] with a spinel structure). SEM images of Co_3O_4 nanoparticles show the spherical agglomerated particles. This is purely due to the magnetic induction of the particles. Optical absorption studies show a blue shift in the energy band gap which reveals the quantum confinement effect. Photoluminescence spectra shows emission peak in the visible region.

Acknowledgement

One of the authors, K. Prema Latha, thanks the UGC-SERO, Hyderabad, India, for awarding the teacher fellowship under Faculty Development Programme vide F. No. FIP-TNMS039/003(TF)/PHYSICS/Ph.D/XII PLAN/2015-16 dated 20 October 2015.

References

- [1] D. Barreca, C. Massignan, S. Daolio, M. Fabrizio, C. Piccirillo, et al., Composition and microstructure of cobalt oxide thin films obtained from a novel cobalt(II) precursor by chemical vapor deposition, *Chem. Mater.* 13 (2001) 588-593.
- [2] J. Liu, D. Wang, M. Wang, D. Kong, Yi Zhang, et al., Uniform two-dimensional Co_3O_4 porous sheets: facile synthesis and enhanced photocatalytic performance, *Chem. Eng. Technol.* 39 (2016) 891-898.
- [3] W.L. Roth, Magnetic properties of normal spinels with only a-a interactions, *Jour. Phys.* 25 (1964) 507-515.
- [4] Xiong Wang, Xiangying Chen, Lisheng Gao, Huagui Zheng, Zude Zhang, Yitai Qian, One-dimensional arrays of Co_3O_4 nanoparticles: synthesis, characterization, and optical and electrochemical properties, *J. Phys. Chem. B* 108 (2004) 16401-16404.
- [5] Lin Guo, Qunjian Huang, Xiao-yuan Li, Shihe Yang, Iron nanoparticles: Synthesis and applications in surface enhanced Raman scattering and electrocatalysis, *Phys. Chem. Chem. Phys.* 3 (2001) 1661-1665.
- [6] S. Vijayakumar, A. Kiruthika Ponnalagi, S. Nagamuthu, G. Muralidharan, Microwave assisted synthesis of Co_3O_4 nanoparticles for high-performance supercapacitors, *Electrochim. Acta* 106 (2013) 500-505.
- [7] R. Manigandan, K. Giribabu, R. Suresh, L. Vijayalakshmi, A. Stephen, V. Narayanan, Cobalt oxide nanoparticles: characterization and its electrocatalytic activity towards nitrobenzene, *Chem. Sci. Trans.* 2 (2013) S47-S50.
- [8] Cordula Gruttner, Joachim Teller, New types of silica-fortified magnetic nanoparticles as tools for molecular biology applications, *J. Magn. Magn. Mater.* 194 (1999) 8-15.
- [9] John Dallas Donaldson, Detmar Beyersmann, Cobalt and cobalt compounds, *Ullmann's Encyclopedia of industrial chemistry*, Wiley-VCH Verlag GmbH & Co. KGaA, Weinheim, 2012, pp. 429-464.
- [10] W.L. Smith, A.D. Hobson, The structure of cobalt oxide, Co_3O_4 , *Acta Cryst.* B29 (1973) 362-363.
- [11] K.F. Wadekar, K.R. Nemade, S.A. Waghuley, Chemical synthesis of cobalt oxide (Co_3O_4) nanoparticles using co-precipitation method, *Res. J. Chem. Sci.* 7 (2017) 53-55.
- [12] R. Sivakami, S. Dhanuskodi, R. Karvembu, Estimation of lattice strain in nanocrystalline RuO_2 by Williamson-Hall and size-strain plot methods, *Spectrochim. Acta Part A: Mol. Biomol. Spect.* 152 (2016) 43-50.
- [13] Q. Jiang, L.H. Liang, D.S. Zhao, Lattice contraction and surface stress of fcc nanocrystals, *J. Phys. Chem. B* 105 (2001) 6275-6277.
- [14] Jagriti Pal, Pratima Chauhan, Study of physical properties of cobalt oxide (Co_3O_4) nanocrystals, *Mater. Charact.* 61 (2010) 575-579.
- [15] G.K. Williamson, R.E. Smallman, Dislocation densities in some annealed and cold-worked metals from measurements on the X-ray Debye-Scherrer spectrum, *Philos. Mag: J. Theo. Expt. App. Phys.* 1 (1956) 34-46.
- [16] G.K. Williamson, W.H. Hall, X-ray line broadening from fcc aluminium and wolfram, *Acta Metall.* 1 (1953) 22-31.
- [17] B. Pejova, A. Isahi, M. Najdoski, I. Grozdanov, Fabrication and characterization of nanocrystalline cobalt oxide thin films, *Mater. Res. Bull.* 36 (2001) 161-170.
- [18] S. Farhadi, M. Javanmard, G. Nadri, Characterization of cobalt oxide nanoparticles prepared by the thermal decomposition, *Acta Chim. Slov.* 63 (2016) 335-343.
- [19] N.J. Tharayil, R. Raveendran, A.V. Vaidyan, P.G. Chithra, Optical, electrical and structural studies of nickel-cobalt oxide nanoparticles, *Indian J. Eng. Mater. Sci.* 15 (2008) 489-496.
- [20] S.A. Makhlof, Z.H. Bakr, K.I. Aly, M.S. Moustafa, Structural, electrical and optical properties of Co_3O_4 nanoparticles, *Superlattices Microstruct.* 64 (2013) 107-117.
- [21] Feng Gu, Chunzhong Li, Yanjie Hu, Ling Zhang, Synthesis and optical characterization of Co_3O_4 nanocrystals, *J. Cryst. Growth.* 304 (2007) 369-373.
- [22] Reem Al-Tuwirqi, A.A. Al-Ghamdi, Nadia Abdel Aal, Ahmad Umar, W.E. Mahmoud, Facile synthesis and optical properties of Co_3O_4 nanostructures by the microwave route, *Superlattice Microstruct.* 49 (2011) 416-421.
- [23] T. Koutzarova, S. Kolev, Ch. Ghelev, D. Paneva, I. Nedkov, Microstructural study and size control of iron oxide nanoparticles produced by micro emulsion technique, *Phys. Stat. Sol.* 5 (2006) 1302-1307.